Summertime C$_1$-C$_5$ alkyl nitrates over Beijing, northern China: Spatial distribution, regional transport, and formation mechanisms

Jingjing Sun[a], Zeyuan Li[a], Likun Xue[a,*], Tao Wang[b], Xinfeng Wang[a], Jian Gao[c], Wei Nie[d], Isobel J. Simpson[e], Rui Gao[c], Donald R. Blake[e], Fahe Chai[c], Wenxing Wang[a,c]

[a] Environment Research Institute, Shandong University, Ji'nan, Shandong, China
[b] Department of Civil and Environmental Engineering, Hong Kong Polytechnic University, Hong Kong, China
[c] Chinese Research Academy of Environmental Sciences, Beijing, China
[d] Joint International Research Laboratory of Atmospheric and Earth System Sciences, School of Atmospheric Sciences, Nanjing University, Nanjing, Jiangsu, China
[e] Department of Chemistry, University of California at Irvine, Irvine, CA, USA
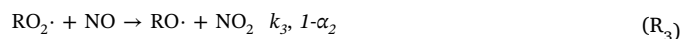
ARTICLE INFO

ABSTRACT

Alkyl nitrates (RONO$_2$) are an important class of nitrogen oxides reservoirs in the atmosphere and play a key role in tropospheric photochemistry. Despite the increasing concern for photochemical air pollution over China, the knowledge of characteristics and formation mechanisms of alkyl nitrates in this region is limited. We analyzed C$_1$-C$_5$ alkyl nitrates measured in Beijing at a polluted urban site in summer 2008 and at a downwind rural site in summers of both 2005 and 2008. Although the abundances of NO$_x$ and hydrocarbons were much lower at the rural site, the mixing ratios of RONO$_2$ were comparable between both sites, emphasizing the regional nature of alkyl nitrate pollution. Regional transport of urban plumes governed the elevated RONO$_2$ levels at the rural site. The concentrations of C$_1$-C$_2$ RONO$_2$ were significantly higher at the rural site in 2008 compared to 2005 despite a decline in NO$_x$ and anthropogenic VOCs, mainly owing to enhanced contributions from biogenic VOCs. The photochemical formation regimes of RONO$_2$ were evaluated by both a simplified sequential reaction model and a detailed master chemical mechanism box model. The observed C$_4$-C$_5$ RONO$_2$ levels can be well explained by the photochemical degradation of n-butane and n-pentane, while the sources of C$_1$-C$_3$ RONO$_2$ were rather complex. In addition to the C$_1$-C$_3$ alkanes, biogenic VOCs and reactive aromatics were also important precursors of methyl nitrate, and alkenes and long-chain alkanes contributed to the formation of C$_2$-C$_3$ RONO$_2$. This study provides insights into the spatial distribution, inter-annual variation and photochemical formation mechanisms of alkyl nitrate pollution over the Beijing area.

1. Introduction

Alkyl nitrates (RONO$_2$) are an important class of organic nitrates in the troposphere, and play key roles in the atmospheric carbon and nitrogen cycles (Bertman et al., 1995; Clemitshaw et al., 1997; Russo et al., 2010), and aerosol formation (Yan et al., 2016). They serve as temporary reservoirs of nitrogen oxides (NO$_x$ = NO + NO$_2$) due to their low reactivity and slow photolysis rate in the troposphere (Atkinson et al., 2006; Jenkin and Clemitshaw, 2000; Seinfeld et al., 1998). In the polluted urban and industrial atmospheres, formation of alkyl nitrates generally consumes NO$_x$ and may result in a negative contribution to ozone (O$_3$) production (Ling et al., 2016), but in the rural and remote areas, alkyl nitrates can act as a potential supplier of NO$_x$ and thus can enhance O$_3$ formation (Aruffo et al., 2014; Day et al., 2003). Therefore, alkyl nitrates have a potential to affect atmospheric chemistry and O$_3$ formation at a regional scale.
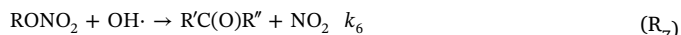
In the troposphere, alkyl nitrates are mainly produced by photochemical reactions of hydrocarbons (RH) and NO$_x$, and their major sinks include photolysis reactions, oxidation by OH, and dry deposition (Russo et al., 2010; Wu et al., 2011). The detailed chemical processes of alkyl nitrates can be described by the following reactions:

$$RH + OH\cdot \rightarrow R\cdot + H_2O \quad k_1, \alpha_1 \tag{R_1}$$

$$R\cdot + O_2 \rightarrow RO_2\cdot \quad k_2 \tag{R_2}$$

$$RO_2\cdot + NO \rightarrow RO\cdot + NO_2 \quad k_3, 1\text{-}\alpha_2 \tag{R_3}$$

$$RO_2\cdot + NO \rightarrow RONO_2 \quad k_4, \alpha_2 \tag{R_4}$$

$$RO\cdot + NO_2 \rightarrow RONO_2 \quad k_5 \tag{R_5}$$

$$RONO_2 + hv \rightarrow RO\cdot + NO_2 \quad J(RONO2) \tag{R_6}$$

$$RONO_2 + OH\cdot \rightarrow R'C(O)R'' + NO_2 \quad k_6 \tag{R_7}$$

where, k_i is the reaction rate constant, and α_i is the branching ratio of the reactions. It should be noted that alkyl nitrates are mainly formed via the reactions of alkyl peroxy radicals (RO_2) with NO (R_4), whereas R_5 is not likely the major source of alkyl nitrates under normal atmospheric conditions (Simpson et al., 2002). In addition to secondary formation, marine emission is also proposed as an important source of methyl nitrate ($MeONO_2$) and ethyl nitrate ($EtONO_2$), especially in the coastal areas (Blake et al., 2003; Chuck et al., 2002; Simpson et al., 2006), and biomass burning is another source of alkyl nitrates (Simpson et al., 2002). Understanding the sources of alkyl nitrates presents a crucial aspect of atmospheric chemistry research.

The relationship between $RONO_2$ and their direct parent hydrocarbons (c.a., methyl nitrate vs. CH_4, ethyl nitrate vs. C_2H_6, etc.) can provide valuable information about the photochemical processing of air masses. Bertman et al. (1995) developed a simplified sequential reaction model to examine the photochemical evolution of alkyl nitrates. The measured ratios of $RONO_2/RH$ can be compared with the theoretical values calculated using laboratory kinetic data to assess the photochemical age of air masses and to diagnose the potential existence of additional sources of alkyl nitrates. If the measured ratios agree well with the theoretical values, it suggests that alkyl nitrates are mainly formed from the oxidation of their direct parent hydrocarbons (i.e., C_1-C_5 alkanes); otherwise it indicates the presence of other sources such as photochemical reactions of hydrocarbons other than C_1-C_5 alkanes if the measured ratios exceed the theoretical ones. This approach has been widely used in many previous studies (Ling et al., 2016; Reeves et al., 2007; Russo et al., 2010; Simpson et al., 2006; Wang et al., 2013; Worton et al., 2010). Nonetheless, this method cannot directly identify the additional precursor species to which the formation of $RONO_2$ is the most sensitive. It is of much interest and necessity to directly identify the individual precursor species of alkyl nitrates and quantify their relationships from both atmospheric chemistry and air quality management points of view.

In recent years, photochemical air pollution has become a major environmental concern in China (Wang et al., 2017; Xue et al., 2014). Despite the increasing concern about photochemical pollutants such as O_3 and peroxyacetyl nitrate (PAN), only limited studies have focused on the characteristics and sources of alkyl nitrates in China. Wang et al. (2013) measured C_1-C_4 alkyl nitrates and investigated their relationships with parent hydrocarbons, carbonyls and O_3 in 47 Chinese cities. Ling et al. (2016) and Lyu et al. (2015) examined the spatiotemporal

variability and photochemical formation processes of C_1-C_5 alkyl nitrates in Hong Kong. In this study, we analyzed the measurement data of C_1-C_5 alkyl nitrates, hydrocarbons, O_3, NO_x and NO_y collected at a polluted urban site and a downwind rural site in Beijing in the summers of 2005 and 2008. The spatial distribution and temporal variations of alkyl nitrates and their parent hydrocarbons were evaluated. In addition to the sequential reaction model, we also utilized the Master Chemical Mechanism (MCM) model to directly identify the precursor species and quantify the $RONO_2$-precursor relationships. Overall, this study provides some insights into the characteristics and formation mechanisms of alkyl nitrates and photochemical pollution in the polluted atmospheres of Beijing.

2. Methods

2.1. Sampling sites

To achieve a better understanding of the photochemical processes on a regional scale, two study sites, representing typical polluted urban and rural areas of Beijing, were carefully selected. The urban site was located at the Chinese Research Academy of Environmental Science (CRAES; 40°2′N, 116°25′E), which is approximately 15 km to the north of Tiananmen square and close to the 5th ring road (Fig. 1). The site was set up on the rooftop of a three-story building with an altitude of ~15 m above the ground level. The details of this site have been described elsewhere (Wang et al., 2010). The measurements were conducted from 10 July to 27 September 2008, during which the 29th Olympic Games was hosted in Beijing and strict anti-pollution measures were implemented (Wang et al., 2010).

The rural site was located in a mountainous area in Changping district (40°22′ N, 116°18′ E; 280 m above sea level), about 50 km northwest of the city center (Fig. 1). The instruments were installed in an orchard growing many kinds of fruit trees such as peach and apricot. There is sparse population and few anthropogenic emissions near the study site. Under the influence of the summer Asian monsoon, the Changping site was usually located downwind of downtown Beijing with the prevailing southerly winds. A detailed description of this study site has been provided previously (Wang et al., 2006). Two phases of intensive measurements were carried out during 28 June – 31 July 2005 and 10 July – 25 August 2008, respectively. The 2008 rural campaign was in parallel with the observations made at CRAES, facilitating an analysis of regional distribution of alkyl nitrates and hydrocarbons over Beijing, and the two phases of measurements at Changping in 2005 and 2008 promoted an evaluation of the inter-
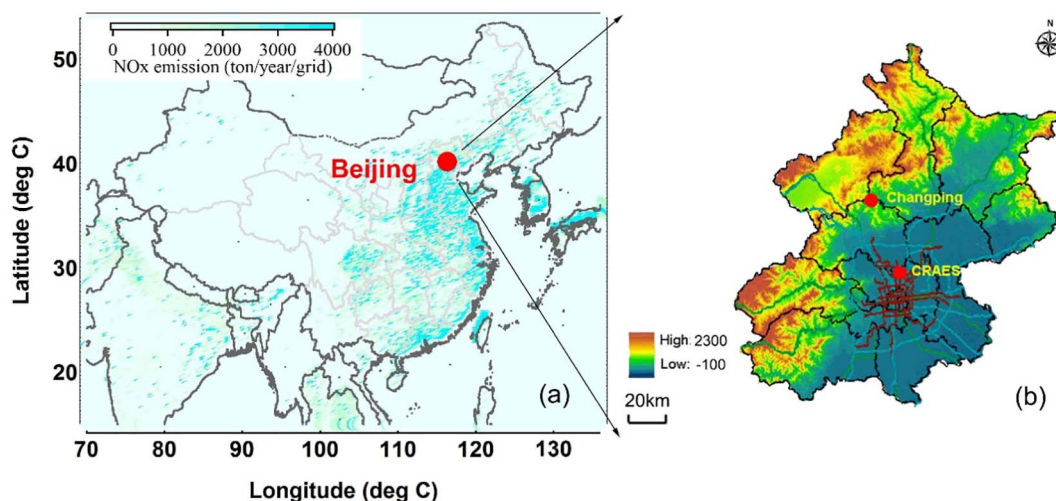

Fig. 1. Maps showing (a) the study area and anthropogenic NO_x emissions (Zhang et al., 2009) and (b) the locations of the two study sites in Beijing. CRAES is the urban site and Changping is the rural site.

Table 1
Summary of chemical compositions and meteorological parameters observed at the rural Changping site in 2005 and 2008, and the urban CRAES site in 2008[a].

Species/meteorological parameters	Changping 05		Changping 08		CRAES 08		P (t-test)	
	Mean ± stdev	Range	Mean ± stdev	Range	Mean ± stdev	Range	Changping 05vs08	08 CPvsCRAES
$MeONO_2$	5.0 ± 2.7	1.6–14.5	11.6 ± 5.3	4.8–29.9	12.3 ± 4.7	3.9–30.8	< 0.01	0.14
$EtONO_2$	9.5 ± 4.8	2.5–24.2	29.4 ± 17.3	8.1–96.4	29.7 ± 13.9	7.2–78.7	< 0.01	0.44
i-$PrONO_2$	23.7 ± 15.2	4.0–71.0	24.9 ± 16.5	4.8–88.7	26.2 ± 14.1	5.7–69.1	0.3	0.25
n-$PrONO_2$	3.6 ± 2.3	0.5–10.6	3.6 ± 2.4	0.8–12.8	3.9 ± 2.0	0.8–10.4	0.4	0.18
2-$BuONO_2$	27.9 ± 21.4	2.7–96.5	40.2 ± 31.5	4.2–162.3	42.5 ± 27.9	6.3–133.0	< 0.01	0.28
3-Me-2-$BuONO_2$	–	–	15.5 ± 11.9	0.9–58	17.2 ± 10.7	1.8–59.0	–	0.12
2-$PeONO_2$	14.3 ± 12.0	1.0–56.2	11.9 ± 9.5	0.9–48.5	13.5 ± 8.8	1.7–41.4	0.12	0.11
3-$PeONO_2$	8.9 ± 7.2	0.7–33.3	7.7 ± 5.8	0.8–28.7	8.2 ± 5.2	1.2–24.8	0.15	0.23
Methane (ppmv)	1.9 ± 0.1	1.8–2.2	2.0 ± 0.1	1.8–2.5	2.2 ± 0.4	1.9–4.5	< 0.01	< 0.01
Ethane	2530 ± 1371	730–5659	2476 ± 1216	762–6315	3418 ± 1783	950–8810	0.42	< 0.01
Propane	1436 ± 1111	118–4302	1337 ± 1029	152–4269	2183 ± 1625	256–7994	0.32	< 0.01
n-Butane	848 ± 849	34–4746	789 ± 708	49–4488	1529 ± 1097	116–5347	0.34	< 0.01
n-Pentane	577 ± 919	13–6377	297 ± 270	14–1751	596 ± 413	54–1957	< 0.05	< 0.01
i-Pentane	1300 ± 2698	67–19,309	1157 ± 394	27–40,440	1809 ± 132	177–11,565	0.26	0.05
Benzene	1395 ± 1248	33–6925	785 ± 613	53–4358	1263 ± 721	99–3778	< 0.01	< 0.01
n-Hexane	210 ± 187	3–660	253 ± 924	7–9359	334 ± 255	24–1571	0.32	0.19
n-Heptane	84 ± 79	6–330	62 ± 136	4–1349	122 ± 85	7–423	0.11	< 0.01
2,3-Dimethylbutane	167 ± 147	3–557	112 ± 111	14–804	230 ± 136	26–716	0.01	< 0.01
Ethene	1281 ± 1153	124–5528	1161 ± 929	134–5915	2026 ± 1371	285–7664	0.24	< 0.01
Propene	113 ± 117	20–483	160 ± 237	23–2133	276 ± 228	35–1473	0.05	< 0.01
1-Butene	52 ± 57	13–259	74 ± 126	7–1192	255 ± 230	32–1540	0.07	< 0.01
i-Butene	113 ± 46	57–248	212 ± 573	22–5496	238 ± 291	39–3083	0.04	0.33
Isoprene	349 ± 156	66–730	742 ± 662	39–4763	1540 ± 1259	32–7591	< 0.01	< 0.01
α + βPinene	46 ± 34	18–167	82 ± 88	5–465	27 ± 34	4–248	< 0.01	< 0.01
m + p-Xylene	392 ± 427	22–2004	144 ± 203	3–1472	590 ± 491	70–2919	< 0.01	< 0.01
o-Xylene	144 ± 136	3–570	43 ± 59	3–480	178 ± 153	14–908	< 0.01	< 0.01
Ethyne	2150 ± 1137	94–5504	1834 ± 1164	146–5195	2788 ± 1592	224–7613	0.08	< 0.01
Toluene	1227 ± 1097	53–4133	718 ± 1435	19–12,372	1699 ± 1535	174–12,341	< 0.01	< 0.01
Ethylbenzene	229 ± 203	11–702	147 ± 149	3–1065	452 ± 336	49–1857	< 0.01	< 0.01
O_3 (ppbv)	60 ± 34	8–286	47 ± 25	7–174	43 ± 30	1–191	< 0.01	< 0.01
NO_x (ppbv)	–	–	2.6 ± 1.8	0.2–15.8	16.2 ± 11.9	1.3–89.7	–	< 0.01
NO_y (ppbv)	13.8 ± 9.4	0.9–58.5	12.0 ± 9.4	0.4–44.6	27.0 ± 14.9	2.5–106.5	< 0.01	< 0.01
T(°C)	25.4 ± 3.8	18.0–36.3	24.4 ± 3.6	15.8–34.1	25.7 ± 4.1	16.9–35.2	< 0.01	< 0.01
RH (%)	66 ± 21	12–94	83 ± 16	26–100	64 ± 18	20–94	< 0.01	< 0.01
Solar radiation(W/m²)	206 ± 266	2–956	169 ± 241	1–927	158 ± 214	0–784	< 0.01	0.09

[a] Units are pptv otherwise specified.

annual differences and effectiveness of the control measures during the Olympic Games.

2.2. Measurement techniques

In the present study, ambient whole air samples were collected in evacuated 2-Liter stainless-steel canisters for the measurements of C_1-C_5 alkyl nitrates and C_1-C_{10} hydrocarbons. Sampling was made at least once per day in the afternoon (12:00–16:00 local time; LT) on clean days, and up to seven times every two hours throughout the daytime (07:00–19:00 LT) on pollution episode days (Wang et al., 2010). A total of 50, 106 and 152 samples were taken at Changping in 2005 and 2008 and at CRAES in 2008, respectively. After the sampling, the canisters were shipped to the University of California at Irvine for chemical analyses using gas chromatography (GC) separation coupled with flame ionization detection (FID), electron capture detection (ECD) and mass spectrometer detection (Colman et al., 2001; Wang et al., 2010). Seven $RONO_2$ species ($MeONO_2$, $EtONO_2$, 1-$PrONO_2$, 2-$PrONO_2$, 2-$BuONO_2$, 2-$PeONO_2$ and 3-$PeONO_2$) were quantified in 2005, while eight species (with addition of 3-Me-2-$BuONO_2$) were detected with a slightly different analytical procedure in 2008. The detection limit was 0.02 pptv for alkyl nitrates and 3 pptv for the non-methane hydrocarbons (NMHCs). The precision was 5% for alkyl nitrates and 3% for most NHMCs.

Ozone was measured with a commercial UV photometric analyzer (TEI, Model 49i). Nitric oxide (NO) and total nitrogen oxides (NO_y = NO + NO_2 + NO_3 + N_2O_5 + HONO + HNO_3 + NO_3^- + PANs + alkyl nitrates) were measured by a commercial chemiluminescence analyzer (TEI, Model 42CY) with an externally placed molybdenum oxide catalytic converter (Wang et al., 2010). Nitrogen dioxide (NO_2) was monitored by another chemiluminescence analyzer (TEI, Model 42i) equipped with a blue light converter (Xu et al., 2013). Ambient temperature, pressure, relative humidity (RH), wind speed and direction, and solar radiation were measured by a set of commercial meteorological sensors at each station (Wang et al., 2010).

2.3. Master chemical mechanism (MCM) model

An observation-based chemical box model (OBM) was used to assess the sensitivity of alkyl nitrate formation to their hydrocarbon precursors. The model is built on the newest version of the Master Chemical Mechanism (MCM v3.3.1) that explicitly describes the degradation of 143 primary VOCs together with the latest IUPAC inorganic nomenclature (Jenkin and Clemitshaw, 2000; Jenkin et al., 2015; Saunders et al., 2003), and has been applied in many previous studies to unravel several essential aspects of atmospheric photochemistry, such as O_3 and PAN formation, reactive chlorine chemistry, and radical chemistry (e.g., Xue et al., 2016; and references therein).

The model was prescribed to a mean condition for the photochemical pollution episodes during which multiple VOC samples were collected. The base model was initialized by the measured average concentrations of C_1-C_5 alkyl nitrates in the early morning and was constrained in real-time by the average diurnal profiles of O_3, CO, SO_2, NO, C_1-C_{10} hydrocarbons, temperature, pressure and RH, to simulate the daytime formation of $RONO_2$. All the measurement data were averaged or interpolated to 1-h concentrations and used as the model inputs. For the nighttime period when VOC data were not available, we
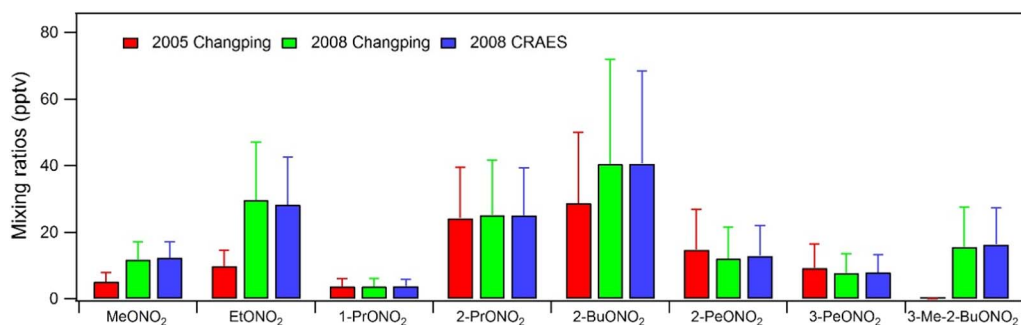
Fig. 2. Average chemical speciation of C_1-C_5 alkyl nitrates during the three measurement campaigns in Beijing. The error bars represent the standard deviations.

assumed constant VOC levels and used the average values of the VOC measurements at 19:00 LT. Such treatment of nighttime VOC input data should not affect the daytime photochemistry simulation results. The model was run for 24 h from 7:00 AM LT. Before each simulation, the model pre-ran for four days with constraints of the campaign-average data so that the model approached a steady state for the unmeasured species (mainly for radicals). The model output of the fifth run was then used for the final analyses.

In addition to the base run, sensitivity modeling studies with 50% reductions of target hydrocarbon species were conducted to estimate the sensitivity of $RONO_2$ production to their precursors. In the present study, the 50+ measured C_1-C_{10} hydrocarbons were classified into 6 categories, namely, parent alkanes (PA; methane for $MeONO_2$, ethane for $EtONO_2$, propane for 1-$PrONO_2$ and 2-$PrONO_2$, n-butane for 2-$BuONO_2$, i-pentane for 3-Me-2-$BuONO_2$, and n-pentane for 2-$PeONO_2$ and 3-$PeONO_2$), alkanes with ≥ 4 carbons (C4HC), alkenes, reactive aromatics (R-AROM; comprising all measured aromatics except benzene), low-reactivity hydrocarbons (LRHC, including acetylene and benzene) and biogenic hydrocarbons (BHC; including isoprene and α/β-pinenes). Relative incremental reactivity (RIR), a metric commonly used to diagnose O_3 formation regimes (Cardelino and Chameides, 1995), was adopted analogously to estimate the $RONO_2$-precursor relationships. It is defined here as the ratio of decrease (in percentage) in model-simulated peak mixing ratios of $RONO_2$ to the decrease in the precursors concentrations (in percentage). The hydrocarbon species with higher positive RIR values are the precursors to which the alkyl nitrate formation is most sensitive.

3. Results and discussion

3.1. Chemical speciation and spatiotemporal variations

Table 1 summarizes the statistics of measurement data of alkyl nitrates, major hydrocarbons, O_3, NO_x, NO_y and meteorological parameters obtained in Beijing during summertime of 2005 and 2008. The average chemical speciation of the observed C_1-C_5 alkyl nitrates is presented in Fig. 2. During the three measurement campaigns, serious photochemical air pollution was observed at both CRAES and Changping sites. For example, the maximum hourly O_3 concentrations were recorded at 286 ppbv at Changping in 2005 and at 191 and 174 ppbv at CRAES and Changping in 2008, respectively. Detailed analyses of O_3 pollution and formation regimes have been documented in our previous publications (Wang et al., 2006; Wang et al., 2010), and we focus on the alkyl nitrates in the present study. The measured average mixing ratios ($\pm$ SD) of summed C_1-C_5 alkyl nitrates were 93 $\pm$ 9, 147 $\pm$ 12 and 146 $\pm$ 13 pptv at Changping in 2005 and at CRAES and Changping in 2008, respectively (recall that the 2005 campaign does not include 3-Me-2-$BuONO_2$, which may account for a small part of the difference). Such levels of ambient alkyl nitrates are among the highest records obtained elsewhere from previous pollution studies, such as Alabama, USA (51 pptv for C_2-C_5 $RONO_2$ in summer 1988; Bertman

et al., 1995), Hong Kong (78 pptv at Tai O in 2001–2002, Simpson et al., 2006; 83 pptv at Tai Mo Shan and 90 pptv at Tsuen Wan in summer 2010, Ling et al., 2016) and Beijing in summer 2011 (109 pptv for C_1-C_4 $RONO_2$; Wang et al., 2013). During our study, 2-$BuONO_2$ was the most abundant $RONO_2$ species at both sites, accounting for 26–28% of the total measured C_1-C_5 $RONO_2$, followed by 2-$PrONO_2$ (17–27%), $EtONO_2$ (12–22%), 2-$PeONO_2$ (8–14%), 3-Me-2-$BuONO_2$ (10–11%) and $MeONO_2$ (6–10%), 3-$PeONO_2$ (5–9%) and 1-$PrONO_2$ (3–4%) only presented a minor contribution to the measured alkyl nitrates.

We compared the measurement data at Changping and CRAES in 2008 to illustrate the regional distribution of photochemical air pollution in Beijing. As expected, the levels of photochemical precursors, i.e., NO_x and various hydrocarbons, were substantially higher at CRAES than at Changping ($p < 0.01$; see Table 1). This is attributed to the extensive fresh emissions in the urban area and photochemical processing of air masses during transport to the rural areas. However, the average mixing ratios of C_1-C_5 alkyl nitrates were comparable at the two sites ($p > 0.1$) even though the abundances of their parent alkanes at Changping were much lower than at CRAES. This is consistent with the regional transport of urban plumes from Beijing to the rural site considering the relatively low reactivity and long lifetime of alkyl nitrates as well as the photochemical formation of alkyl nitrates during transport. Furthermore, the average mixing ratio of O_3 at Changping (47 $\pm$ 25 ppbv) was higher than at CRAES (43 $\pm$ 30 ppbv; $p < 0.01$). The above comparison clearly demonstrates the regional nature of photochemical air pollution and alkyl nitrate formation over the Beijing area.

We also compared the measurement results at Changping in both 2005 and 2008 to examine the inter-annual changes of alkyl nitrate pollution and/or assess the effects of anti-pollution measures commenced during the Olympic Games in 2008. Overall, the ambient concentrations of NO_y and most anthropogenic hydrocarbons at Changping in 2008 were lower than those observed in 2005 (although the differences for some VOC species are not statistically significant). However, the most reactive compounds such as isoprene and C_3-C_4 alkenes had higher levels in 2008 compared to 2005 (Table 1). Such difference should be due to the irregular emissions around the study site given the short lifetimes of these species. For secondary pollutants, the O_3 pollution levels in 2008 (47 $\pm$ 25 ppbv) was lower than in 2005 (60 $\pm$ 34 ppbv). In comparison, C_3-C_5 alkyl nitrates did not significantly change between 2005 and 2008, except for 3-$PeONO_2$ that showed a slight decrease due to the significant decline of n-pentane ($p < 0.05$; Table 1). Moreover, $MeONO_2$ (11.6 $\pm$ 5.3 pptv vs. 5.0 $\pm$ 2.7 pptv), $EtONO_2$ (29.4 $\pm$ 17.3 pptv vs. 9.5 $\pm$ 4.8 pptv) and 2-$BuONO_2$ (40.2 $\pm$ 31.5 pptv vs. 27.9 $\pm$ 21.4 pptv) were higher in 2008 than in 2005 ($p < 0.01$). Examination of VOC data showed a slight or moderate decrease in the abundances of the direct $RONO_2$ precursors (i.e., C_2-C_5 alkanes) but an increase of biogenic hydrocarbons (i.e., isoprene and α/β-pinenes; $p < 0.01$) from 2005 to 2008, implying the important role of biogenic emissions in the photochemical formation of alkyl nitrates in 2008. We will analyze in detail the photochemical formation mechanisms of alkyl nitrates in Section 3.4.
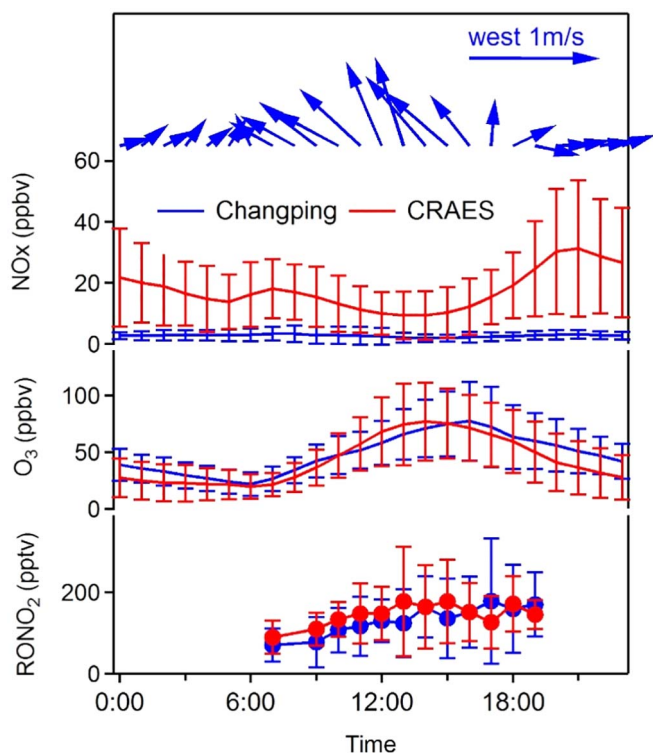
Fig. 3. Average diurnal variations of alkyl nitrates, O_3, NO_x and wind sectors at CRAES (in red) and Changping (in blue) in 2008. Error bars are the standard errors of the measurements. (For interpretation of the references to colour in this figure legend, the reader is referred to the web version of this article.)

3.2. Effect of regional transport

Fig. 3 shows the average diurnal profiles of alkyl nitrates, O_3, NO_x and wind sectors observed at CRAES and Changping in 2008. It clearly displays the well-defined daytime formation of O_3 and alkyl nitrates with broad concentration peaks in the afternoon. The amplitudes of O_3 and alkyl nitrate daytime accumulation were comparable between both sites, confirming again the nearly uniform regional distribution of photochemical pollution over Beijing. The maximum values of O_3 and alkyl nitrates at Changping occurred approximately two hours later than at CRAES, which in combination with the prevailing southerly winds during the daytime indicate the transport of urban plumes from downtown to the rural areas. Therefore, regional transport of urban pollution played an important role in the observed O_3 and alkyl nitrates at the Changping site.

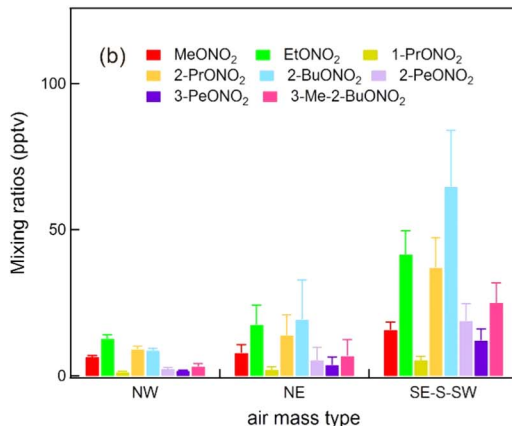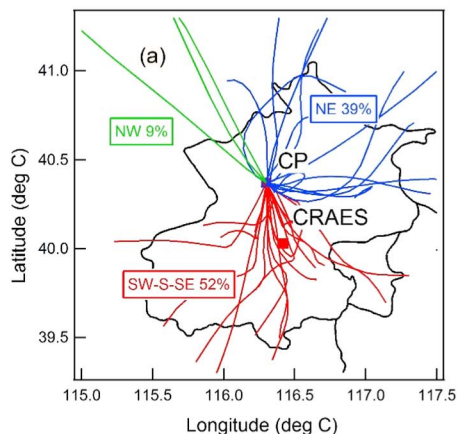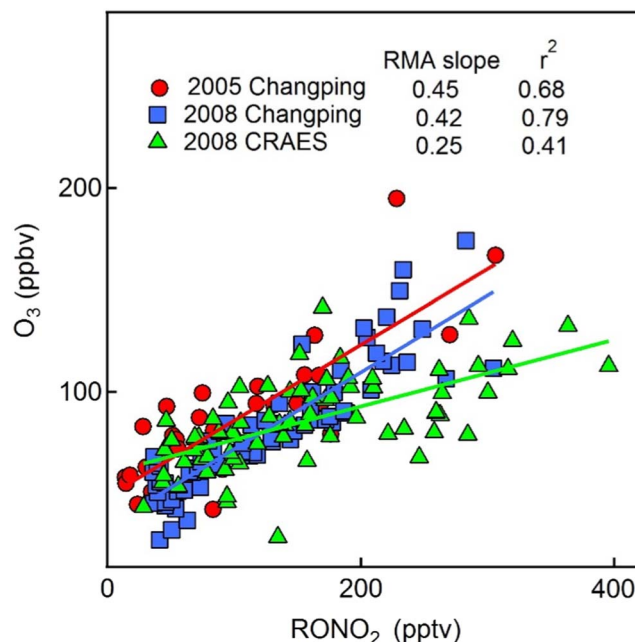To further elucidate the effect of regional transport on the alkyl

Fig. 5. Scatter plots of O_3 versus alkyl nitrates at Changping and CRAES.

nitrate pollution, we calculated the 12-h backward trajectories arriving at Changping at an altitude of 350 m above ground level (Fig. 4). Trajectories were computed once per day (at 13:00 LT) from 11 July to 25 August 2008, using the NOAA ARL HYSPLIT model with the Global Data Assimilation System (GDAS) meteorological data (Stein et al., 2016). Air masses arriving at Changping can be easily divided into three categories according to the origins and transport routes of their back trajectories. Air masses coming from the south sector and passing over downtown Beijing dominated the air flow, with an average fraction of 52%, followed by those from the northeast (39%) and northwest sectors (9%). The average concentrations of C_1-C_5 $RONO_2$ compositions in the different air mass categories are also shown in Fig. 4. As expected, the air masses from the south sector contained the highest levels of alkyl nitrates. Indeed, the photochemical O_3 pollution episodes observed at Changping were mainly ascribed to the transport of urban plumes from downtown Beijing and/or the further upwind North China Plain region (Wang et al., 2010).

3.3. Relationships with O_3 and PAN

Alkyl nitrates, O_3 and peroxyacetyl nitrate (PAN) are co-products of atmospheric photochemical reactions of NO_x and VOCs. Fig. 5 shows the scatter plots of the measured alkyl nitrates versus O_3 concentrations

Fig. 4. (a) 12-h backward trajectories arriving at Changping during 11 July - 25 August 2008; (b) distributions of C_1-C_5 $RONO_2$ in the three types of air masses.
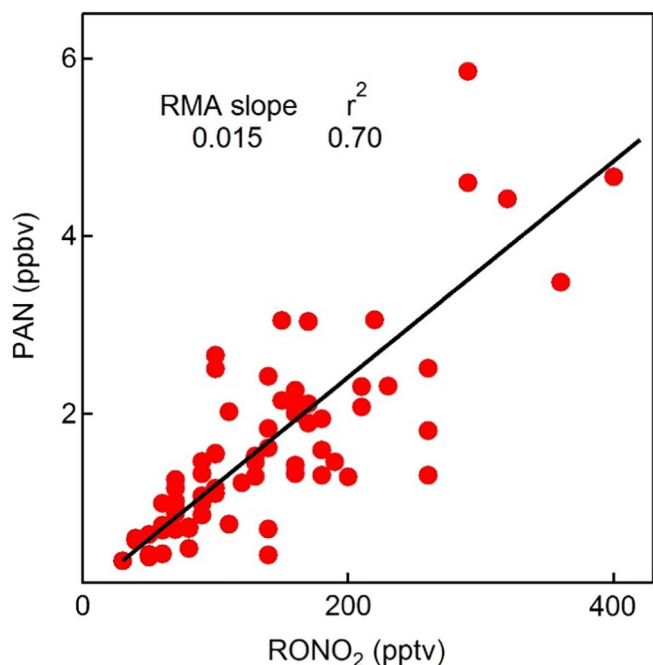
Fig. 6. Scatter plots of alkyl nitrates versus PAN at CRAES in 2008.

at both Changping and CRAES during summer 2005 and 2008. Moderate to strong positive correlation can be clearly seen, with correlation coefficients (r^2) of 0.41–0.79. The reduced major axis (RMA) slopes of O_3 versus $RONO_2$ were 0.25 ppbv/pptv at CRAES in 2008, and 0.45 and 0.42 ppbv/pptv at Changping in 2005 and 2008, respectively. This means that approximately 25–45 ppbv of O_3 could be formed along with each 100 pptv of alkyl nitrates being photochemically produced in Beijing. Thus, alkyl nitrates can also be used to infer the O_3 formation potential at a given location (e.g., Simpson et al., 2006).

Fig. 6 presents the positive correlation ($r^2 = 0.70$) between alkyl nitrates and PAN, both of which were concurrently observed at CRAES in 2008. The RMA slope of PAN versus $RONO_2$ was 0.015 ppbv/pptv, indicating that about 1.5 ppbv of PAN was produced along with each 100 pptv of alkyl nitrates being photochemically formed. Indeed, PAN

has much higher photochemical production efficiency than alkyl nitrates, and usually composes a higher fraction of the oxidized nitrogen oxides (i.e., NO_z) in urban environments (Liu et al., 2010).

3.4. Photochemical formation mechanisms of alkyl nitrates

Photochemical oxidation of parent hydrocarbons is a vital source of alkyl nitrates. As mentioned above, a simplified sequential reaction model has been developed by Bertman et al. (1995) to examine the relationship between alkyl nitrates and their direct parent hydrocarbons, which has been widely applied to diagnose the presence of additional precursors of $RONO_2$ other than parent alkanes (Ling et al., 2016; Russo et al., 2010; Wang et al., 2013). The ratio of a target $RONO_2$ to its parent hydrocarbon ($RONO_2/RH$) in an air parcel with a certain photochemical age is determined by the initial $RONO_2/RH$ ratio, photochemical formation of $RONO_2$, and degradation of both $RONO_2$ and RH. By assuming that RO_2 radicals mainly react with NO in high NO_x environments (cross reactions of peroxy radicals are considered to be less important) and the reaction of hydrocarbon with OH is the rate-limiting step for the $RONO_2$ production, the $RONO_2/RH$ ratio can be calculated as a function of photochemical processing time (t) according to the following expression (Bertman et al., 1995):

$$\frac{RONO_2}{RH} = \frac{\beta k_A}{k_B - k_A}(1 - e^{(k_A - k_B)t}) + \frac{[RONO_2]_0}{[RH]_0}e^{(k_A - k_B)t} \quad (E1)$$

$$\beta = \alpha_1\alpha_2$$

where, k_A and k_B represent the production and destruction rate constants of alkyl nitrates ($k_A = k_{1*}[OH]$, $k_B = k_{6*}[OH] + J_{RONO_2}$), and k_1 and k_6 are the rate constants for reactions of RH and $RONO_2$ with OH. α_1 and α_2 are the branching ratio of Reaction (R_1) and product yield of $RONO_2$ from Reaction (R_4), the values of which were taken from Kwok and Atkinson (1995), Atkinson and Arey (2003), and Bertman et al. (1995). The OH concentration is a key parameter and was not measured in the present study, and we adopted a daytime average value of 1×10^7 molecule cm^{-3} according to the OH measurements available in suburban Beijing (Lu et al., 2013). J_{RONO2} is the photolysis frequency of alkyl nitrates, and was obtained from the literatures (Bertman et al., 1995; Wang et al., 2013; and references therein). $[RONO_2]_0/[RH]_0$ is the initial ratio of $RONO_2/RH$, and was approximated by the average
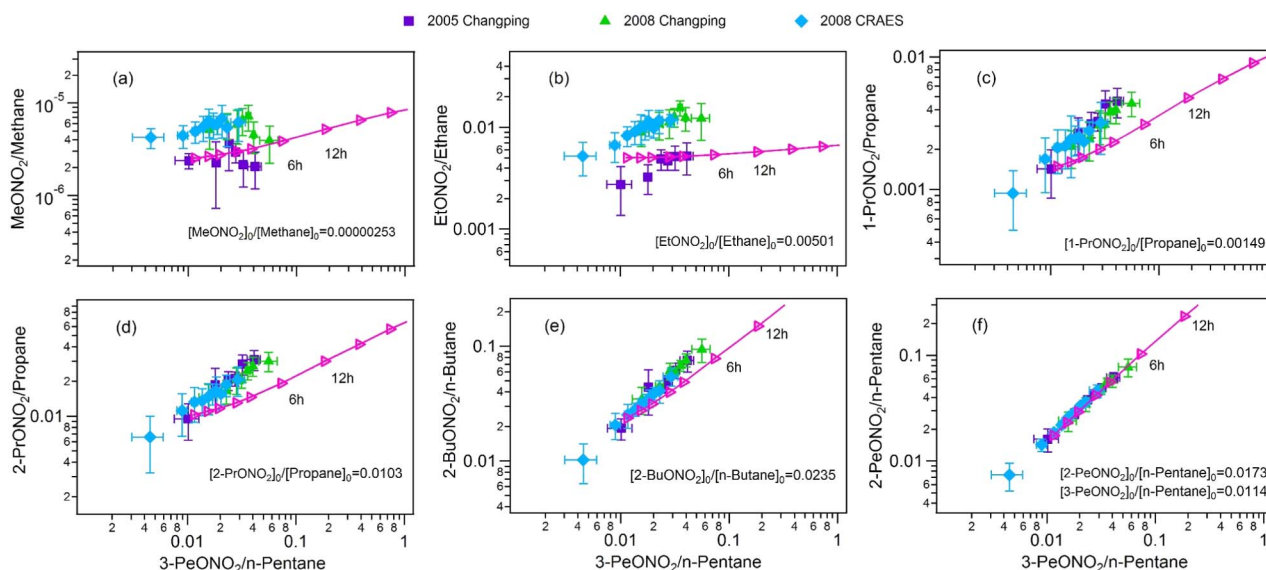

Fig. 7. Relationships of C_1-C_5 $RONO_2/RH$ versus 3-PeONO$_2$/n-pentane at Changping and CRAES: (a) MeONO$_2$/methane, (b) EtONO$_2$/ethane, (c) 1-PrONO$_2$/propane, (d) 2-PrONO$_2$/propane, (e) 2-BuONO$_2$/n-butane, (f) 2-PeONO$_2$/n-pentane. The pink lines with triangles are the theoretical photochemical curves. $[RONO_2]_0/[RH]_0$ was calculated as the average of the background (lowest 10th percentile) ratio values at the two sites. (For interpretation of the references to colour in this figure legend, the reader is referred to the web version of this article.)
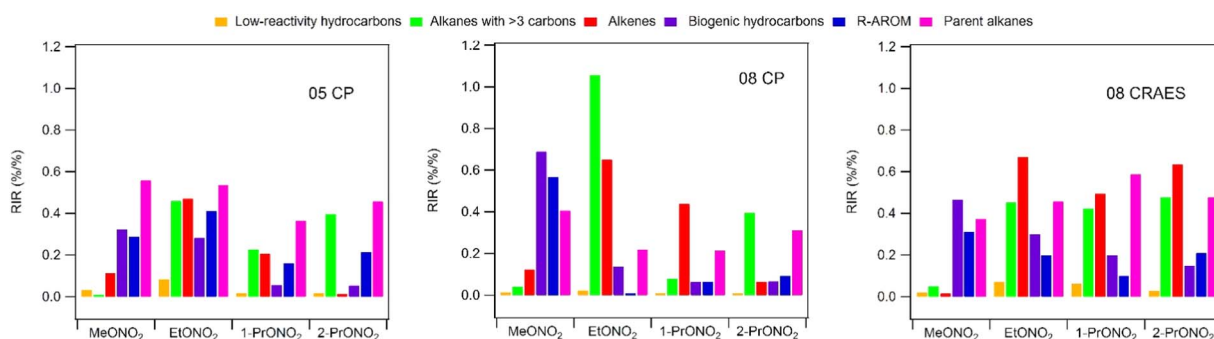
Fig. 8. The OBM-calculated RIRs of major hydrocarbon groups for C_1-C_3 RONO$_2$ at Changping and CRAES.

values of the lowest measured 10% RONO$_2$/RH ratios during the individual measurement campaigns. Solving Eq. (E1) gives a photochemical curve of the RONO$_2$/RH ratio along with the air mass age.

Fig. 7 shows the scatter plots of the observed individual RONO$_2$/RH ratios versus 3-PeONO$_2$/n-pentane and comparison with the calculated theoretical photochemical curves. The 3-PeONO$_2$/n-pentane ratio was chosen as a reference because the formation of long-chain alkyl nitrates is usually dominated by a single source. Specifically, 3-PeONO$_2$ in the atmosphere is exclusively formed from the oxidation of n-pentane via abstraction of a hydrogen atom from the central carbon by OH (Sommariva et al., 2008). As shown in Fig. 7, the photochemical ages of most air masses observed in the present study fell in the range of 1–6 h, and the air at Changping was generally 2 h more aged than that at CRAES. This agrees well with the finding that the Changping site was greatly influenced by the regional transport of urban plumes from downtown Beijing. For C_4-C_5 alkyl nitrates (i.e., 2-BuONO$_2$ and 2-PeONO$_2$), the measured RONO$_2$/RH ratios lie fairly close to or on the calculated photochemical curves, indicating that the formation of these compounds can be well explained by their parent alkanes, namely, n-butane and n-pentane. This is consistent with the knowledge that longer chain alkyl nitrates usually have fewer sources (or precursors; Sommariva et al., 2008). In contrast, different results were obtained for the C_1-C_3 alkyl nitrates. In summer 2005, the observed MeONO$_2$/methane and EtONO$_2$/ethane ratios at Changping were generally quite close to the predicted photochemical curves, showing the dominant role of methane and ethane as the primary precursors. In comparison, during the summer of 2008 the observed ratios of MeONO$_2$/methane and EtONO$_2$/ethane at both Changping and CRAES were much higher than the theoretical values, suggesting the contributions from additional sources such as oxidation of hydrocarbons other than methane and ethane. As for 1-PrONO$_2$ and 2-PrONO$_2$, the observed ratios during all three campaigns were higher than the photochemical curves, which indicated the presence of other VOC precursors besides propane. Overall, the above analysis reveals different characteristics of the alkyl nitrate formation in 2005 and 2008, and points to the complex sources of short-chain alkyl nitrates in Beijing, especially in the summer of 2008.

We further assessed the relationships between C_1-C_3 alkyl nitrates and different types of hydrocarbons by using the MCM model as described in Section 2.3. All the measured 50 + hydrocarbon species were classified into six major categories, namely, PA, BHC, R-AROM, alkenes, C4HC and LRHC (as described in Section 2.3). A series of sensitivity modeling analyses with 50% reduction in the target hydrocarbon group were conducted to compute the relative incremental reactivity (RIR) values, and the results are presented in Fig. 8. In summer 2005, parent alkanes showed the highest RIRs for all the C_1-C_3 RONO$_2$, highlighting the dominant contribution of parent alkanes to the alkyl nitrate formation at Changping. In summer 2008, in contrast, parent alkanes did not show the largest RIR values for the C_1-C_3 RONO$_2$, although they still showed important contributions. The methyl nitrate formation was most sensitive to biogenic VOCs, followed by reactive aromatics and

parent hydrocarbons at both Changping and CRAES. The photochemical degradation of isoprene and aromatic VOCs produce an amount of methyl peroxy radical (CH$_3$O$_2$) as an intermediate, which then reacts with NO to form methyl nitrate. At high NOx conditions, the reactions of CH$_3$O with NO$_2$ may be also an important formation pathway of methyl nitrate (Simpson et al., 2006; Archibald et al., 2007). In addition, degradation of isoprene and aromatics also yields an amount of other ROx radicals, which may indirectly prompt the formation of alkyl nitrates. For ethyl nitrate, alkanes with ≥4 carbons showed the highest RIR, followed by alkenes at Changping. Alkenes and alkanes with ≥4 carbons were also the major precursors for ethyl nitrate at CRAES. The photochemical degradation of alkenes and alkanes with ≥4 carbons forms ethyl peroxy radical (C$_2$H$_5$O$_2$), which can react with NO to form ethyl nitrate. Alkenes and alkanes with ≥4 carbons were also the most significant contributors to the photochemical formation of C_3 RONO$_2$ (1-PrONO$_2$ and 2-PrONO$_2$) at Changping and CRAES. Overall, in addition to the parent alkanes, biogenic VOCs and reactive aromatics potentially contributed to the formation of methyl nitrate, while longer chain alkanes and alkenes may result in the formation of C_2-C_3 alkyl nitrates.

We should note that the observational data analyzed in the present study were obtained in 2005 and 2008, almost ten years ago. Long-term measurements have indicated a 37% decline of the NMHC mixing ratios in Beijing from 2004 to 2012, although the anthropogenic emission inventory estimation suggested an increase of 28% during the same period (Wang et al., 2015). However, the observed NMHC decrease in Beijing was mainly contributed by the significant reduction of vehicle emissions, whilst the VOC emissions from solvent usage and industry did not show significant temporal changes (Wang et al., 2015). Reactive aromatics are important components of industrial solvents. Moreover, there are not effective control measures for biogenic emissions to date. Therefore, our findings based on such a relatively old data set can still provide useful information to support the formulation of control strategy towards photochemical pollution in Beijing.

4. Summary

We analyzed three sets of measurement data of C_1-C_5 alkyl nitrates and related parameters collected at both urban and rural sites in Beijing in summers of 2005 and 2008. Elevated concentrations of alkyl nitrates were observed along with high O$_3$ mixing ratios, indicating the serious photochemical pollution status over Beijing. The alkyl nitrate levels were comparable at both sites even though the abundances of NO$_x$ and VOCs were much lower at the rural site. Regional transport of urban plumes played an important role in the observed pollution levels at the rural site. The C_1-C_2 alkyl nitrates measured at the rural site in 2008 were significantly higher than in 2005, despite a decrease in some anthropogenic VOCs. The increase in biogenic VOCs in 2008 may explain this difference. Photochemical oxidation of n-butane and n-pentane dominated the formation of C_4-C_5 alkyl nitrates, whilst the C_1-C_3 species showed more complex sources. In addition to the direct parent

alkanes, biogenic VOCs and reactive aromatics may significantly contribute to $MeONO_2$ formation, and alkenes and longer chain alkanes are potential precursors of C_2-C_3 alkyl nitrates. This study reveals the spatial distribution and inter-annual variation of photochemical air pollution, and helps clarify the photochemical formation regimes of alkyl nitrates in Beijing.

Acknowledgements

References

Archibald, A.T., Khan, M.A.H., Watson, L.A., Clemitshaw, K.C., Utembe, S.R., Jenkin, M.E., et al., 2007. Comment on 'long-term atmospheric measurements of C–C alkyl nitrates in the Pearl River Delta region of southeast China' by Simpson et al. Atmos. Environ. 41, 7369–7370.

Aruffo, E., Di Carlo, P., Dari-Salisburgo, C., Biancofiore, F., Giammaria, F., Busilacchio, M., et al., 2014. Aircraft observations of the lower troposphere above a megacity: alkyl nitrate and ozone chemistry. Atmos. Environ. 94, 479–488.

Atkinson, R., Arey, J., 2003. Atmospheric degradation of volatile organic compounds. Chem. Rev. 103, 4605–4638.

Atkinson, R., Baulch, D., Cox, R., Crowley, J., Hampson, R., Hynes, R., et al., 2006. Evaluated kinetic and photochemical data for atmospheric chemistry: volume II–gas phase reactions of organic species. Atmos. Chem. Phys. 6, 3625–4055.

Bertman, S.B., Roberts, J.M., Parrish, D.D., Buhr, M.P., Goldan, P.D., Kuster, W.C., et al., 1995. Evolution of alkyl nitrates with air mass age. J. Geophys. Res.-Atmos. 100, 22805–22813.

Blake, N.J., Blake, D.R., Swanson, A.L., Atlas, E., Flocke, F., Rowland, F.S., 2003. Latitudinal, vertical, and seasonal variations of C_1-C_4 alkyl nitrates in the troposphere over the Pacific Ocean during PEM-Tropics A and B: oceanic and continental sources. J. Geophys. Res. Atmos. 108, 171–181.

Cardelino, C.A., Chameides, W.L., 1995. An observation-based model for analyzing ozone precursor relationships in the urban atmosphere. J. Air Waste Manage. Assoc. 45, 161–180.

Chuck, A.L., Turner, S.M., Liss, P.S., 2002. Direct evidence for a marine source of C_1 and C_2 alkyl nitrates. Science 297, 1151–1154.

Clemitshaw, K.C., Williams, J., Rattigan, O.V., Shallcross, D.E., Law, K.S., Cox, R.A., 1997. Gas-phase ultraviolet absorption cross-sections and atmospheric lifetimes of several C_2–C_5 alkyl nitrates. J. Photochem. Photobiol., A 102, 117–126.

Colman, J.J., Swanson, A.L., Meinardi, S., Sive, B.C., Blake, D.R., Rowland, F.S., 2001. Description of the analysis of a wide range of volatile organic compounds in whole air samples collected during PEM-Tropics A and B. Anal. Chem. 73, 3723–3731.

Day, D.A., Dillon, M.B., Wooldridge, P.J., Thornton, J.A., Rosen, R.S., Wood, E.C., et al., 2003. On alkyl nitrates, O_3, and the "missing NO_y". J. Geophys. Res. Atmos. 108 (D16), 4501.

Jenkin, M.E., Clemitshaw, K.C., 2000. Ozone and other secondary photochemical pollutants: chemical processes governing their formation in the planetary boundary layer. Atmos. Environ. 34, 2499–2527.

Jenkin, M.E., Young, J.C., Rickard, A.R., 2015. The MCM v3.3.1 degradation scheme for isoprene. Atmos. Chem. Phys. Discuss. 15, 9709–9766.

Kwok, E.S.C., Atkinson, R., 1995. Estimation of hydroxyl radical reaction rate constants for gas-phase organic compounds using a structure-reactivity relationship: an update. Atmos. Environ. 29, 1685–1695.

Ling, Z., Guo, H., Simpson, I.J., Saunders, S.M., Lam, S.H.M., Lyu, X., et al., 2016. New insight into the spatiotemporal variability and source apportionments of C_1–C_4 alkyl nitrates in Hong Kong. Atmos. Chem. Phys. 16, 8141–8156.

Liu, Z., Wang, Y., Gu, D., Zhao, C., Huey, L.G., Stickel, R., et al., 2010. Evidence of reactive aromatics as a marjor source of peroxyl acetyl nitrate over China. Environ. Sci. Technol. 44, 7017–7022.

Lu, K.D., Hofzumahaus, A., Holland, F., Bohn, B., Brauers, T., Fuchs, H., et al., 2013. Missing OH source in a suburban environment near Beijing: observed and modelled OH and HO_2 concentrations in summer 2006. Atmos. Chem. Phys. 13, 1057–1080.

Lyu, X.P., Ling, Z.H., Guo, H., Saunders, S.M., Lam, S.H.M., Wang, N., et al., 2015. Re-examination of C_1-C_5 alkyl nitrates in Hong Kong using an observation-based model. Atmos. Environ. 120, 28–37.

Reeves, C.E., Slemr, J., Oram, D.E., Worton, D., Penkett, S.A., Stewart, D.J., et al., 2007. Alkyl nitrates in outflow from North America over the North Atlantic during intercontinental transport of ozone and precursors 2004. J. Geophys. Res. Atmos. 112, 409–427.

Russo, R., Zhou, Y., Haase, K., Wingenter, O., Frinak, E., Mao, H., et al., 2010. Temporal variability, sources, and sinks of C_1-C_5 alkyl nitrates in coastal New England. Atmos. Chem. Phys. 10, 1865–1883.

Saunders, S.M., Jenkin, M.E., Derwent, R.G., Pilling, M.J., 2003. Protocol for the development of the master chemical mechanism, MCM v3 (part a): tropospheric degradation of non-aromatic volatile organic compounds. Atmos. Chem. Phys. 3, 181–193.

Seinfeld, J.H., Pandis, S.N., Noone, K., 1998. Atmospheric chemistry and physics: from air pollution to climate change. Phys. Today 51, 88–90.

Simpson, I.J., Meinardi, S., Blake, D.R., Blake, N.J., Rowland, F.S., Atlas, E., et al., 2002. A biomass burning source of C_1-C_4 alkyl nitrates. Geophys. Res. Lett. 29, 21-1–21-4.

Simpson, I.J., Wang, T., Guo, H., Kwok, Y., Flocke, F., Atlas, E., et al., 2006. Long-term atmospheric measurements of C_1-C_5 alkyl nitrates in the Pearl River Delta region of southeast China. Atmos. Environ. 40, 1619–1632.

Sommariva, R., Trainer, M., de Gouw, J.A., Roberts, J.M., Warneke, C., Atlas, E., et al., 2008. A study of organic nitrates formation in an urban plume using a master chemical mechanism. Atmos. Environ. 42, 5771–5786.

Stein, A.F., Draxler, R.R., Rolph, G.D., Stunder, B.J.B., Cohen, M.D., Ngan, F., 2016. NOAA's HYSPLIT atmospheric transport and dispersion modeling system. Bull. Am. Meteorol. Soc. 96, 2059–2077.

Wang, T., Ding, A., Gao, J., Wu, W.S., 2006. Strong ozone production in urban plumes from Beijing, China. Geophys. Res. Lett. 33, 320–337.

Wang, T., Nie, W., Gao, J., Xue, L., Gao, X., Wang, X., et al., 2010. Air quality during the 2008 Beijing Olympics: secondary pollutants and regional impact. Atmos. Chem. Phys. 10, 7603–7615.

Wang, M., Shao, M., Chen, W., Lu, S., Wang, C., Huang, D., et al., 2013. Measurements of C_1–C_4 alkyl nitrates and their relationships with carbonyl compounds and O_3 in Chinese cities. Atmos. Environ. 81, 389–398.

Wang, M., Shao, M., Chen, W., Lu, S., Liu, Y., Yuan, B., et al., 2015. Trends of non-menthane hydrocarbons (NMHC) emissions in Beijing during 2002–2013. Int. Biodeter. Biodegr. 14, 85–94.

Wang, T., Xue, L., Brimblecombe, P., Yun, F.L., Li, L., Zhang, L., 2017. Ozone pollution in China: a review of concentrations, meteorological influences, chemical precursors, and effects. Sci. Total Environ. 575, 1582–1596.

Worton, D.R., Reeves, C.E., Penkett, S.A., Sturges, W.T., Slemr, J., Oram, D.E., et al., 2010. Alkyl nitrate photochemistry during the tropospheric organic chemistry experiment. Atmos. Environ. 44, 773–785.

Wu, Z., Wang, X., Chen, F., Turnipseed, A.A., Guenther, A.B., Niyogi, D., et al., 2011. Evaluating the calculated dry deposition velocities of reactive nitrogen oxides and ozone from two community models over a temperate deciduous forest. Atmos. Environ. 45, 2663–2674.

Xu, Z., Wang, T., Xue, L.K., Louie, P.K.K., Luk, C.W.Y., Gao, J., et al., 2013. Evaluating the uncertainties of thermal catalytic conversion in measuring atmospheric nitrogen dioxide at four differently polluted sites in China. Atmos. Environ. 76, 221–226.

Xue, L., Wang, T., Gao, J., Ding, A., Zhou, X., Blake, D., et al., 2014. Ground-level ozone in four Chinese cities: precursors, regional transport and heterogeneous processes. Atmos. Chem. Phys. 14, 13175–13188.

Xue, L., Gu, R., Wang, T., Wang, X., Saunders, S., Blake, D., et al., 2016. Oxidative capacity and radical chemistry in the polluted atmosphere of Hong Kong and Pearl River Delta region: analysis of a severe photochemical smog episode. Atmos. Chem. Phys. 16, 1–26.

Yan, C., Nie, W., Äijälä, M., Rissanen, M.P., Canagaratna, M.R., Massoli, P., et al., 2016. Source characterization of highly oxidized multifunctional compounds in a boreal Forest environment using positive matrix factorization. Atmos. Chem. Phys. 16, 1–31.

Zhang, Q., Streets, D.G., Carmichael, G.R., He, K.B., Huo, H., Kannari, A., et al., 2009. Asian emissions in 2006 for the NASA INTEX-B mission. Atmos. Chem. Phys. 9, 5131–5153.